Titanium(IV) and Zirconium(IV) Sulfato Complexes Containing the Kläui Tripodal Ligand: Molecular Models of Sulfated Metal Oxide Surfaces

Qian-Feng Zhang,[a] Tony C. H. Lam,[a] Xiao-Yi Yi,[a] Eddie Y. Y. Chan,[a] Wai-Yeung Wong,[b] Herman H. Y. Sung,[a] Ian D. Williams,[a] and Wa-Hung Leung*[a]

Abstract: Treatment of titanyl sulfate in about 60 mM sulfuric acid with NaL_{OEt} ($L_{OEt}^- = [(\eta^5\text{-}C_5H_5)Co\{P(O)(OEt)_2\}_3]^-$) afforded the μ-sulfato complex $[(L_{OEt}Ti)_2(\mu\text{-}O)_2(\mu\text{-}SO_4)]$ (**2**). In more concentrated sulfuric acid (>1 M), the same reaction yielded the di-μ-sulfato complex $[(L_{OEt}Ti)_2(\mu\text{-}O)(\mu\text{-}SO_4)_2]$ (**3**). Reaction of **2** with HOTf (OTf = triflate, CF_3SO_3) gave the tris(triflato) complex $[L_{OEt}Ti(OTf)_3]$ (**4**), whereas treatment of **2** with Ag(OTf) in CH_2Cl_2 afforded the sulfato-capped trinuclear complex $[\{(L_{OEt})_3Ti_3(\mu\text{-}O)_3\}(\mu_3\text{-}SO_4)\{Ag(OTf)\}][OTf]$ (**5**), in which the Ag(OTf) moiety binds to a μ-oxo group in the $Ti_3(\mu\text{-}O)_3$ core. Reaction of **2** in H_2O with $Ba(NO_3)_2$ afforded the tetranuclear complex $(L_{OEt})_4Ti_4(\mu\text{-}O)_6$ (**6**). Treatment of **2** with $[\{Rh(cod)Cl\}_2]$ (cod = 1,5-cyclooctadiene), $[Re(CO)_5Cl]$, and $[Ru(t\text{Bu}_2\text{bpy})(PPh_3)_2Cl_2]$ ($t\text{Bu}_2\text{bpy}$ = 4,4′-di-*tert*-butyl-2,2′-dipyridyl) in the presence of Ag(OTf) afforded the heterometallic complexes $[(L_{OEt})_2Ti_2(O)_2(SO_4)\{Rh(cod)\}_2][OTf]_2$ (**7**), $[(L_{OEt})_2Ti(O)_2(SO_4)\{Re(CO)_3\}][OTf]$ (**8**), and $[\{(L_{OEt})_2Ti_2(\mu\text{-}O)\}(\mu_3\text{-}SO_4)(\mu\text{-}O)_2\{Ru(PPh_3)(t\text{Bu}_2\text{bpy})\}][OTf]_2$ (**9**), respectively. Complex **9** is paramagnetic with a measured magnetic moment of about 2.4 μ_B. Treatment of zirconyl nitrate with NaL_{OEt} in 3.5 M sulfuric acid afforded $[(L_{OEt})_2Zr(NO_3)][L_{OEt}Zr(SO_4)(NO_3)]$ (**10**). Reaction of $ZrCl_4$ in 1.8 M sulfuric acid with NaL_{OEt} in the presence Na_2SO_4 gave the μ-sulfato-bridged complex $[L_{OEt}Zr(SO_4)(H_2O)]_2(\mu\text{-}SO_4)$ (**11**). Treatment of **11** with triflic acid afforded $[(L_{OEt})_2Zr][OTf]_2$ (**12**), whereas reaction of **11** with Ag(OTf) afforded a mixture of **12** and trinuclear $[\{L_{OEt}Zr(SO_4)(H_2O)\}_3(\mu_3\text{-}SO_4)][OTf]$ (**13**). The Zr^{IV} triflato complex $[L_{OEt}Zr(OTf)_3]$ (**14**) was prepared by reaction of $L_{OEt}ZrF_3$ with Me_3SiOTf. Complexes **4** and **14** can catalyze the Diels–Alder reaction of 1,3-cyclohexadiene with acrolein in good selectivity. Complexes **2**–**5**, **9**–**11**, and **13** have been characterized by X-ray crystallography.

Keywords: O ligands · P ligands · sulfates · titanium · zirconium

Introduction

Sulfated metal oxides and related inorganic solid acids[1] have attracted much attention due to their high catalytic activity in the industrially important conversion of hydrocarbons. Of particular significance is sulfated zirconia, which is capable of catalyzing the isomerization of alkanes such as *n*-butane at low temperatures.[1,2] Sulfated zirconia catalysts suffer from a drawback of fast deactivation presumably due to coke formation. The stability and activity of sulfated zirconia are found to be enhanced when a metal promoter, notably Pt, is added and catalytic reactions are carried out under hydrogen.[3] The role of the metal promoter in bifunctional sulfated zirconia catalysts is a subject of debate.[1c] Sulfated zirconia supported organometallic catalysis is well documented. For example, Group 4 and 5 alkyls chemisorbed on sulfated zirconia surfaces were found to exhibit high catalytic activity in arene hydrogenation and alkene polymerization reactions,[4] demonstrating the rich organometallic chemistry of bimetallic $M/SO_4^{2-}/ZrO_2$ systems. To better understand the catalytic chemistry of sulfated zirconia, it is essential to elucidate the structures and reactivity of their active sites at the molecular level. Of particular interest is the nature of sulfur species on sulfated zirconia surfaces. It is generally believed that the sulfate species is covalently bonded to zirconia surfaces and the sulfur oxidation state for the catalysts is +6. In previous studies, surface sulfur

[a] Dr. Q.-F. Zhang, Dr. T. C. H. Lam, X.-Y. Yi, Dr. E. Y. Y. Chan, Dr. H. H. Y. Sung, Prof. Dr. I. D. Williams, Prof. Dr. W.-H. Leung
Department of Chemistry
The Hong Kong University of Science and Technology
Clear Water Bay, Kowloon, Hong Kong (China)
Fax: (+852) 2358-1594
E-mail: chleung@ust.hk

[b] Prof. Dr. W.-Y. Wong
Department of Chemistry
Hong Kong Baptist University
Waterloo Road, Kowloon, Hong Kong (China)

 DOI: 10.1002/chem.200400853

species such as bidentate sulfate **1a** with two S=O groups, tridentate sulfate **1b** with one S=O group, and bisulfate HSO_4^- **1c** have been proposed for sulfated zirconia catalysts.[5–8] Nevertheless, the issue as to how metal ions/metal hydrocarbyls interact with the sulfated zirconia active sites, and the mechanisms of organometallic reactions occurring on sulfated zirconia surfaces are not well understood.[8] In this connection, we set out to model sulfated zirconia surfaces by molecular Group 4 sulfato complexes in oxygen ligand environments.

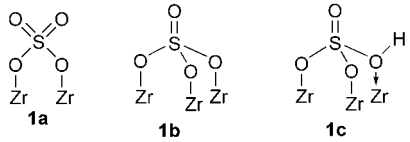

The most extensively studied models of Group 4 metal oxides are homo- and heterometallic compounds with oxygen ligands such as alkoxides,[9] aryloxides,[9a,10] siloxides,[11] silsesquixane,[12] and calixarene macrocycles,[13] as well as organometallic oxo clusters supported by cyclopentadienyl ligands.[14,15] However, molecular Group 4 sulfato compounds with oxygen ligands are uncommon. Examples of structurally characterized Ti^{IV} sulfato complexes include the cyclopentadienyl compounds $[\{Cp_3^*Ti_3(\mu\text{-}SO_4)Cl\}(\mu\text{-}O)_3]$[16] and $[Cp_2Ti(\mu\text{-}SO_4)Ti(H_2O)Cp_2]$[17] ($Cp=\eta^5\text{-}C_5H_5$, $Cp^*=\eta^5\text{-}C_5Me_5$). Toward this end, sulfated zirconia models based on Group 4 sulfato complexes containing the Kläui oxygen tripodal ligand, $[CpCo\{P(O)(OR)_2\}_3]^-$ (denoted as L_{OR}^-, R = alkyl)[18] were prepared and investigated. Owing

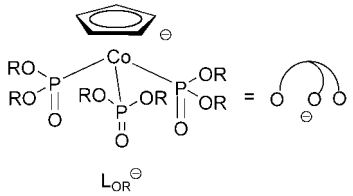

to the high affinity of Ti and Zr for the P=O group, reactions of Zr^{IV} and Ti^{IV} compounds with L_{OR}^- in organic solvents were reported to afford the bis(tripod) compounds $[(L_{OR})_2M]^{2+}$ readily.[19–21] Half-sandwich $[(L_{OR})MCl_3]$ compounds (M = Ti, Zr) were prepared by reaction of NaL_{OEt} with $[CpZrCl_3]$[20] or $[Ti(O\mathit{i}Pr)_2Cl_2]/HCl$.[21] Previously, we found that in aqueous media titanyl and zirconyl compounds could be stabilized by L_{OEt}^-, and the resulting $L_{OEt}M^{IV}(aq)$ species abstract fluoride from HBF_4 to give $L_{OEt}MF_3$.[21] In the absence of a fluoride-containing ligand, reaction of zirconyl nitrate with NaL_{OEt} yielded tetranuclear $[(L_{OEt})_4Zr_4(\mu_3\text{-}O)_2(\mu\text{-}OH)_4(H_2O)_2][NO_3]_4$ that reacted with $[PO_4]^{3-}$ to give trinuclear and tetranuclear μ_3-phosphato cluster compounds.[22] This result demonstrates that it is possible to construct $L_{OEt}M^{IV}$-based cluster compounds with core structures similar to those of metal oxides by condensation of $M^{4+}(aq)$ with L_{OEt}^- in the presence of appropriate oxyanions in water. Herein, we report on the synthesis of dinuclear and trinuclear Ti^{IV} and Zr^{IV} sulfato complexes supported by L_{OEt}^-, the core structures of which are relevant to the proposed sulfated zirconia active sites. A heterometallic complex containing a $Ti_2Ru(\mu\text{-}O)_3(\mu_3\text{-}SO_4)$ core has been isolated and structurally characterized.

Results and Discussion

Ti^{IV} sulfato and triflato complexes: Treatment of titanyl sulfate in H_2SO_4 (60 mM ca. 60 mM) with one equivalent of NaL_{OEt} and Na_2SO_4 gave a yellow solution. Upon extraction with CH_2Cl_2 and recrystallization from CH_2Cl_2–hexane, pale yellow crystals identified as the sulfato-bridged complex $[(L_{OEt}Ti)_2(\mu\text{-}O)_2(\mu\text{-}SO_4)]$ (**2**) were isolated (Scheme 1). When

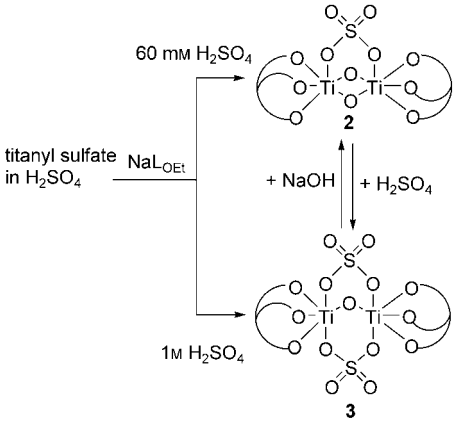

Scheme 1. Preparations of dinuclear Ti sulfato complexes **2** and **3**.

the same reaction was carried out in more concentrated sulfuric acid (>1 M), the di-μ-sulfato-bridged complex $[(L_{OEt}Ti)_2(\mu\text{-}O)(\mu\text{-}SO_4)_2]$ (**3**) was obtained. The IR S=O stretching frequencies for **2** and **3** of 1259 and 1281 cm^{-1}, respectively, are lower than that for $[\{Cp_3^*Ti_3Cl(\mu\text{-}O_2SO_2)\}(\mu\text{-}O)_3]$ (1310 cm^{-1}).[17] The ν_1 vibrational mode[23] for the sulfato ligand could not be assigned due to overlap with the intense signals of the L_{OEt}^- ligand in the 1000–1100 cm^{-1} region. Both **2** and **3** are air stable in organic solvents such as CH_2Cl_2 and acetone, and are easily identified by their characteristic ^{31}P NMR spectra (in $CDCl_3$, for **2**: $\delta=119.0$ (s) ppm; for **3**: $\delta=119.4$ (t), 125.8 (d) ppm). They could be dissolved in water (solubility of ca. 10^{-5} M at room temperature) to give acidic solutions. Addition of $Ba(NO_3)_2$ to **2** or **3** in water resulted in precipitation of $BaSO_4$, indicating that the sulfato ligands of these complexes dissociate in solution. According to ^{31}P NMR spectroscopy, **2** and **3** could be interconverted to each other in aqueous solution (Scheme 1). Solutions of **3** in sulfuric acid at $0.5<pH<3.2$ were found to

contain predominately **2** ($\delta = 123.9$ (t), 131.5 (d) ppm). When the pH was lowered to about 0.5, the conversion of **2** to **3** was found to occur ($\delta = 123.9$ (d), 131.1 (t) ppm). At pH > 4, a new $L_{OEt}Ti^{IV}$ species that exhibited a resonance at $\delta = 122.5$ ppm in the ^{31}P NMR spectrum, which is identical with that of tetranuclear **6** (vide infra), was found.

The solid-state structure of **2** is shown in Figure 1. The structure of **2** consists of a $Ti_2(O)_2$ core with the average Ti–O bond length (1.831(4) Å) and Ti-O-Ti angle (95.3(2)°)

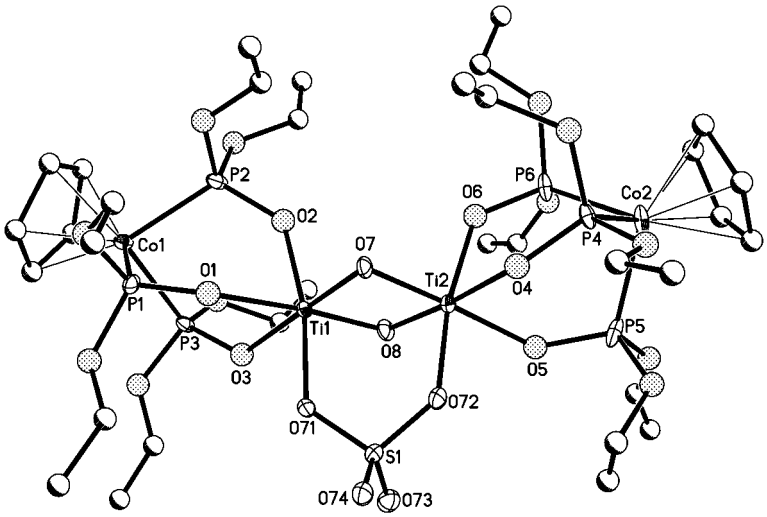

Figure 1. Molecular structure of **2**. The ellipsoids are drawn at 30% probability level. Selected bond lengths [Å] and angles [°]: Ti–O(L_{OEt}) 1.971(4)–2.118(4), Ti1–O7 1.797(4), Ti1–O8 1.845(4), Ti2–O7 1.862(4), Ti2–O8 1.819(4), Ti1–O71 1.994(4), Ti2–O72 1.977(4), Ti1–Ti2 2.7050(13), S1–O71 1.523(4), S1–O72 1.524(5), S1–O73 1.438(5), S1–O74 1.427(5); Ti1-O7-Ti2 95.3(2), Ti1-O8-Ti2 95.2(2), Ti1-O71-S1 127.6(3), Ti2-O72-S1 128.3(3).

that are typical for Ti_2O_2 titanoxane compounds, for example, $[\{Ti(acac)_2\}_2(\mu\text{-}O)_2]$ (Hacac = pentane-2,4-dione).[24] The average Ti–O(SO_4) distance of 1.986(4) Å for **2** is similar to that in $[\{Cp^*_3Ti_3Cl(\mu\text{-}O_2SO_2)\}(\mu\text{-}O)_3]$ (1.953(8) Å).[17] The average Ti–O(L_{OEt}) bond length of 2.036(5) Å for **2** is similar to that in $L_{OEt}TiCl_3$ (1.975(6) Å).[21] Compound **3** has also been characterized by X-ray diffraction (Figure 2). Unlike $[\{L_{OEt}Ti(Cl_4cat)\}_2(\mu\text{-}O)]$ (Cl_4catH_2 = tetrachlorocatechol)[21] compound **3** possesses a bent Ti-O-Ti unit. While the identity of **3** has been confirmed, its bond lengths and angles have not been analyzed given the high *R* values due to the disorder of the structure.

Treatment of **2** with excess triflic acid in CH_2Cl_2 afforded the tris(triflato) complex $[L_{OEt}Ti(OTf)_3]$ (**4**), which was isolated as an air-sensitive orange solid. Alternatively, **4** could be prepared in good yield by the reaction of $[L_{OEt}TiCl_3]$ or $[L_{OEt}Ti(i\text{OPr})_2Cl]$[21] with triflic acid. Complex **4** is soluble in CH_2Cl_2 and THF but insoluble in Et_2O and hexane. The ^{19}F NMR spectrum shows a singlet at $\delta = -77.7$ ppm attributed to the triflato ligands. The structure of **4** is shown in Figure 3. The geometry around Ti is pseudo-octahedral with the average Ti–O(OTf) distance of 1.998(3) Å that is similar to that in $[\{Ti(Ot\text{Bu})(OTf)(H_2O)\}(\mu\text{-}O)(\mu\text{-}OTf)_2]$ (Ti–OTf(terminal) 1.995 Å).[25] The Ti–O(L_{OEt}) bonds in **4** (1.884(3) Å) are apparently shorter than those in $[L_{OEt}TiCl_3]$ (av 1.975(6) Å) and $[L_{OEt}TiF_3]$ (2.020(2) Å),[21] indicating the weak *trans* influence of the triflato ligands.

Heterometallic complexes: Treatment of **2** with Ag(OTf) in CH_2Cl_2 afforded the Ti^{IV}-Ag^I complex $[(L_{OEt})_3Ti_3(\mu\text{-}O)_3(\mu_3\text{-}SO_4)\{Ag(OTf)\}][OTf]$ (**5**) (Scheme 2). On the other hand, sulfate abstraction of **2** by $Ba(NO_3)_2$ in water resulted in precipitation of $BaSO_4$ and the isolation of yellow crystals analyzed as tetranuclear $[(L_{OEt})_4Ti_4O_6]\cdot 1.5\,HNO_3$ (**6**).[26] A preliminary X-ray diffraction study revealed that **6** contains an adamantane-like $Ti_4(\mu\text{-}O)_6$ core similar to that in $[Cp^*_4Ti_4(\mu\text{-}O)_6]$.[27] ^{31}P NMR spectroscopy indicated that the Ag^I-induced conversion of **2** to **5** in $CDCl_3$ is a clean, rapid reac-

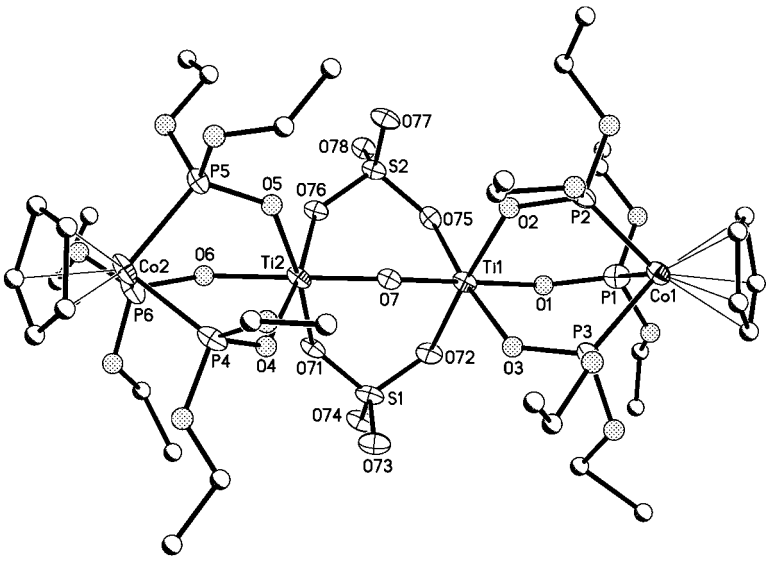

Figure 2. Molecular structure of **3**. The ellipsoids are drawn at 30% probability level.

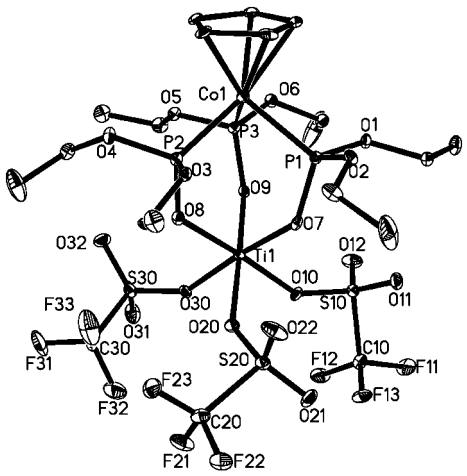

Figure 3. Molecular structure of **4**. The ellipsoids are drawn at 30% probability level. Selected bond lengths [Å] and angles [°]: Ti1–O10 1.985(3), Ti1–O20 2.005(3), Ti1–O30 2.005(3), Ti1–O7 1.878(3), Ti1–O8 1.888(3), Ti1–O9 1.887(2); O10-Ti1-O30 84.35(11), O10-Ti1-O20 89.04(11), O30-Ti1-O20 86.64(11).

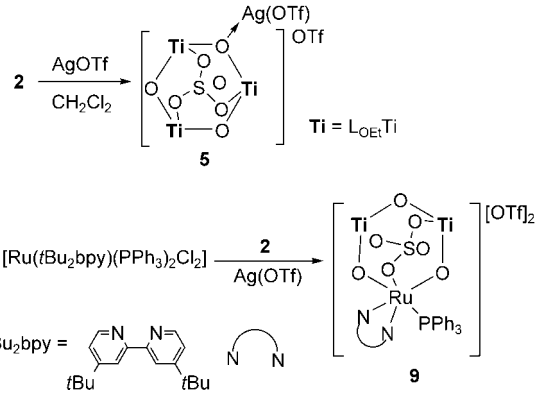

Scheme 2. Preparations of trinuclear Ti suflato complexes **5** and **9**.

tion (<15 min). Although the mechanism for formation of **5** is not clear, it probably involves the combination of **2** with a Ti triflato species, possibly $[(L_{OEt})_2Ti_2(\mu\text{-}O)_2(OTf)_2]$. Indeed, treatment of **2** with **4** in CH_2Cl_2 afforded **5** as the major isolated product. Thus, it appears that the conversion of unsaturated $(L_{OEt})_2Ti_2O_2$ species to the $Ti_3(\mu\text{-}O)_3(\mu_3\text{-}SO_4)$ core in CH_2Cl_2 solution is a favorable, facile process. Complex **5** has been characterized by X-ray crystallography. Transition-metal complexes containing $\mu_3\text{-}SO_4^{2-}$ ligands are rather uncommon.[28] To our knowledge, this is the first structurally characterized Ti μ_3-sulfato complex. It may be noted that reaction of $[\{Cp^*TiCl(\mu\text{-}O)\}_3]$ with Ag_2SO_4 afforded a trinuclear complex $[\{Cp^*_3Ti_3(\mu\text{-}O_2SO_2)Cl\}(\mu\text{-}O)_3]$ containing a bidentate bridging sulfato ligand.[17] The IR S=O stretching frequency for the $\mu_3\text{-}SO_4^{2-}$ group in **5** was determined to be 1265 cm^{-1}, which is similar to those found for $[Cr_4(\mu_4\text{-}O)(\mu_3\text{-}SO_4)_2(\mu\text{-}Cl)_5Cl_4]^{3-}$ (1268 and 1275 cm^{-1}).[28a] The structure of the cation $[(L_{OEt})_3Ti_3(\mu\text{-}O)_3(\mu_3\text{-}SO_4)\{Ag(OTf)\}]^+$ in **5** consists of a $Ti_3(\mu\text{-}O)_3$ core capped by a $\mu_3\text{-}SO_4^{2-}$ ligand (Figure 4). A similar Ti_3O_3 core was found in $[\{Cp^*TiCl(\mu\text{-}O)\}_3]$.[29] However, unlike $[\{Cp^*TiCl(\mu\text{-}O)\}_3]$, the six-membered Ti_3O_3 ring in **5** is nonplanar and has a pseudo-chair conformation (Figure 5). In addition, the Ti–O bond lengths in **5** are not equivalent (average short and long Ti–O distances of 1.795(3) and 1.891(3) Å, respectively), indicative of asymmetrical Ti=O–Ti bridges in the Ti_3O_3 ring. The Ag atom was found to be disordered and was split in two sites, Ag1A and Ag1B, with occupancies of 0.8 and 0.2, respectively. The position of Ag1A is shown in Figure 4. The

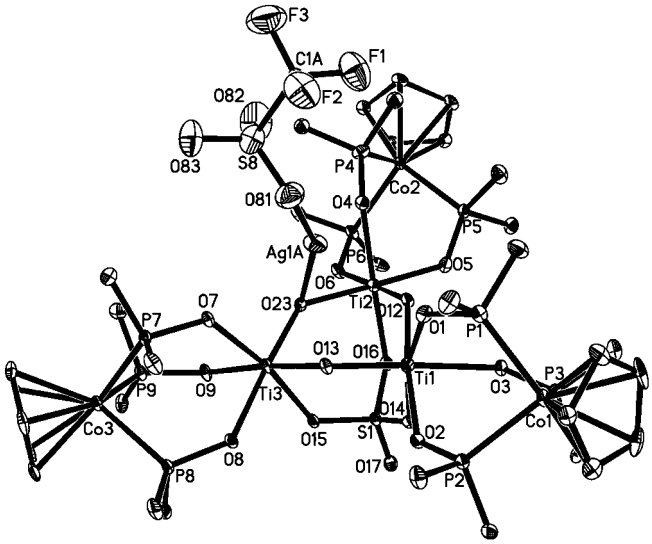

Figure 4. Molecular structure of the cation $[(L_{OEt}Ti)_3(\mu\text{-}O)_3(\mu_3\text{-}SO_4)(AgOTf)]^+$ in **5**. The ellipsoids are drawn at 30% probability level. Selected bond lengths [Å] and angles [°]: Ti–O(L_{OEt}) 1.974(3)–2.085(3), Ti1–O12 1.891(3), Ti1–O13 1.785(3), Ti1–O14 2.014(3), Ti2–O12 1.800(3), Ti2–O16 2.005(3), Ti2–O23 1.887(3), Ti3–O13 1.895(3), Ti3–O15 2.022(3), Ti3–O23 1.799(3), S1–O14 1.487(4), S1–O15 1.492(3), S1–O16 1.495(3), S1–O17 1.413(3); Ti1-013-Ti3 136.8(2), Ti2-O12-Ti1 135.7(2), Ti3-O23-Ti2 136.6(2), S1-O14-Ti1 128.5(2), S1-O15-Ti3 127.9(2), S1-O16-Ti2 128.2(2).

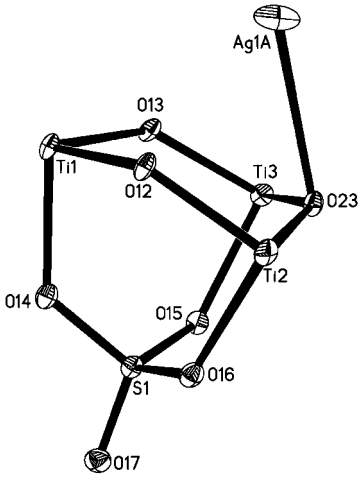

Figure 5. View of the Ti_3O_3 ring in **5** showing the chair conformation.

Ag1A–O23 separation of 2.488(3) Å suggests donor–acceptor-type interactions between the Ag and the μ-oxo group. The average Ti–O(μ_3-SO_4) distance of 2.024(4) Å is slightly longer than the Ti–O(μ-SO_4) distances in **2**. The S–O_t distance of 1.417(5) Å in **5** is significantly shorter than the S–O(Ti) distances (av 1.495(4) Å), consistent with a S=O double bond.

Chloride abstraction of [{Rh(cod)Cl}$_2$] (cod = 1,5-cyclooctadiene) and [Re(CO)$_5$Cl] with Ag(OTf) followed by treatment with **2** afforded the bimetallic complexes [$(L_{OEt})_2$-$Ti_2(O)_2(SO_4)${Rh(cod)}$_2$][OTf]$_2$ (**7**) and [$(L_{OEt})_2Ti_2(O)_2$-(SO_4){Re(CO)$_3$}][OTf] (**8**), respectively, which were characterized by NMR spectroscopy and mass spectrometry. Unfortunately, despite several attempts, we have not been able to obtain X-ray quality crystals to elucidate the coordination modes of the {Rh(cod)} and {Re(CO)$_3$} moieties for the two compounds. It seems probable that the Rh and Re atoms bind to the μ-oxo group(s) in the Ti_3O_3 core. It may be noted that bimetallic complexes [Cp*Ti_3(μ_3-CR)(μ_3-$O)_3${Mo(CO)$_3$}] (R = H or Me), in which the *fac*-Mo(CO)$_3$ moiety binds to the three μ-oxo groups, have been isolated.[15b]

Treatment of **1** with [Ru(*t*Bu$_2$bpy)(PPh$_3$)$_2$Cl$_2$][30] (*t*Bu$_2$bpy = 4,4′-di-*tert*-butyl-2,2′-dipyridyl) in the presence of two equivalents of Ag(OTf) in CH_2Cl_2 afforded a formally Ti^{IV}–Ru^{IV} complex [{$(L_{OEt})_2Ti_2$(μ-O)}(μ_3-SO_4)(μ-$O)_2$[Ru-(*t*Bu$_2$bpy)(PPh$_3$)}][OTf]$_2$ (**9**) (Scheme 2). Although the mechanism for the formation of **9** has not been elucidated, it seems likely that the rearrangement of the dinuclear M_2(μ-$O)_2$(μ-SO_4) to trinuclear M_3(μ-$O)_3$(μ_3-SO_4) core similar to that of **5** is involved. The oxidation of Ru^{II} to Ru^{IV} was probably caused by Ag^I and/or by a Ru disproportionation reaction because **9** was isolated even if the synthesis and workup were carried out under N_2. The FAB mass spectrum shows the parent ion peak at *m*/*z* 1944 corresponding to [*M*−2OTf]$^+$. Compound **9** is paramagnetic with a measured solid-state magnetic moment of about 2.4 μ_B at 298 K, which is less than the spin-only value for two unpaired electrons. The cyclic voltammogram of **9** exhibits a reversible couple at about 0.04 V versus $Cp_2Fe^{+/0}$ (0.1 M [*n*Bu$_4$N][PF_6] in CH_2Cl_2, glassy carbon electrode, scan rate = 100 mV s^{-1}) that is tentatively assigned as the Ru^{IV}/Ru^{III} couple because Ru^{IV}/Ru^{V} couples for oxo-Ru^{IV} complexes with amine ligands are usually found at higher potentials (e.g. 1.39 V versus $Cp_2Fe^{+/0}$ for *trans*-[Ru(py)$_4$(O)Cl]$^+$ (py = pyridine) in MeCN[31]). However, additional evidence is needed to confirm this assignment. The solid-state structure of **9** has been established by X-ray diffraction (Figure 6).

The dication [{$(L_{OEt})_2Ti_2$(μ-O)}(μ_3-SO_4)(μ-$O)_2$[Ru-(*t*Bu$_2$bpy)(PPh$_3$)}]$^{2+}$ contains a Ti_2Ru(μ-$O)_3$ core that is capped by a μ_3-SO_4^{2-} ligand. Alternatively, this dication can be viewed as a six-coordinate Ru^{IV} complex containing a dianionic, tridentate-*fac*-*O*,*O*,*O*(sulfato) [{$(L_{OEt})_2Ti_2$(μ-O)}(μ-$O)_2$(μ_3-SO_4)]$^{2-}$ ligand along with one *t*Bu$_2$bpy and one PPh$_3$. Related neutral, tridentate-*O*,*O*,*O* [Cp*$_3$Ti(μ_3-CR)(μ-O)] (R = H or Me) metalloligands were found in heterometallic cubane complexes [Cp*Ti_3(μ_3-CR)(μ_3-$O)_3${Mo(CO)$_3$}].[15b]

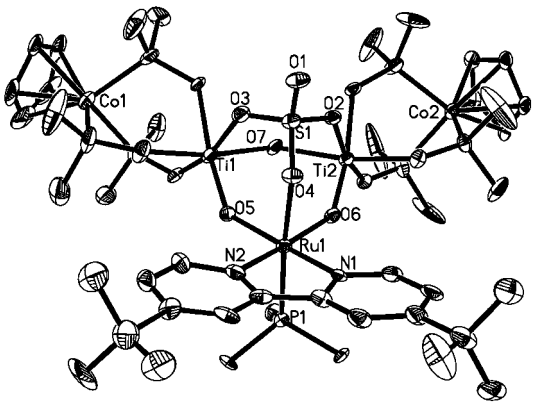

Figure 6. Molecular structure of the dication [{$(L_{OEt})_2Ti_2$(μ-O)}(μ_3-SO_4)-(μ-$O)_2${Ru(PPh$_3$)(*t*Bu$_2$bpy)}]$^{2+}$ in **9**. The ellipsoids are drawn at 30% probability level. Ethyl groups in L_{OEt}^- and phenyl ring in the PPh$_3$ are omitted for clarity. Selected bond lengths [Å] and angles [°]: Ru1–N1 2.049(7), Ru1–N2 2.048(7), Ru1–O4 2.163(5), Ru1–O5 1.973(6), Ru1–O6 1.975(5), Ru1–P1 2.302(2), Ti–O(L_{OEt}) 1.959(6)–2.103(6), Ti1–O3 2.029(6), Ti1–O5 1.732(5), Ti1–O7 2.009(6), Ti2–O2 2.032(6), Ti2–O6 1.719(6), Ti2–O7 2.040(6), S1–O1 1.431(6), S1–O2 1.488(6), S1–O3 1.491(6), S1–O4 1.485(6); O5-Ru1-P1 93.90(18), O6-Ru1-P1 91.45(17), N2-Ru1-P1 95.9(2), N1-Ru1-P1 92.6(2), O4-Ru1-P1 174.98(17), Ti1-O5-Ru1 138.5(3), Ti2-O6-Ru1 140.2(3), Ti1-O7-Ti2 130.8(3).

The Ti–O(Ti) bond (1.719(6) Å) is shorter than the Ti–O(Ru) bonds (av 1.974 Å), while the Ti-O-Ti angle (130.8(3)°) is smaller than the Ti-O-Ru angles (av 139.4(3)°). The long Ru–Ti separations (av 3.469 Å) suggest the absence of direct Ti–Ru interactions. The Ru–O(Ti) distances (av 1.974 Å) are longer than the Ru–O(Ru) distances in [$(L_{OMe})_2Ru_2(H_2O)_2$(μ-$O)_2$][OTf]$_2$ (av 1.918 Å).[32] The average Ru–N (2.049(7) Å) and Ru–P (2.302(2) Å) distances are slightly shorter than those of the Ru^{II} compound [Ru(Me$_2$bpy)(PPh$_3$)$_2$(C≡C*t*Bu)Cl] (2.086 and 2.359 Å, respectively).[30]

Z^{IV} sulfato and triflato complexes: Treatment of zirconyl nitrate in ca. 3.5 M sulfuric acid with NaL_{OEt} in the presence of excess Na_2SO_4 afforded [$(L_{OEt})_2Zr(NO_3)$][$L_{OEt}Zr(NO_3)_2$-(SO_4)] (**10**) (Scheme 3). Despite the high sulfate concentration in the reaction mixture, it was not possible to displace all nitrato ligands from Zr. It may be noted that depending upon experimental conditions reaction of zirconyl nitrate with NaL_{OEt} in nitric acid led to the isolation of [(L_{OEt})Zr-$(NO_3)_3$], [$(L_{OEt})_2Zr(NO_3)$][NO_3], or [$(L_{OEt})_4Zr_4$(μ_3-$O)_2$(μ-$OH)_4(H_2O)_2$][NO_3]$_4$.[22] The ^{1}H NMR spectrum of **10** shows two Cp proton resonances at δ = 5.46 and 5.42 ppm, consistent with the solid-state structure. The IR spectrum shows a

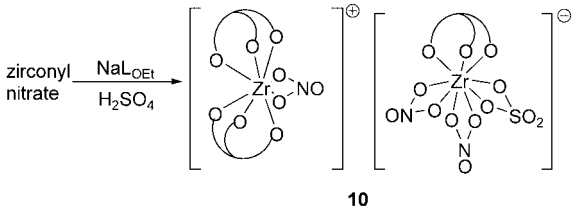

10

Scheme 3. Preparation of **10**.

peak at 1305 cm^{-1} that is assigned as the N=O stretch of the chelating nitrato ligand. The S=O stretching frequency for the chelating sulfato ligand was observed at 1248 cm^{-1}. The solid-state structures of the complex cation and anion in **10** are shown in Figure 7 and Figure 8, respectively. In the complex cation $[(L_{OEt})_2Zr(NO_3)]^+$, which is identical with that in $[(L_{OEt})_2Zr(NO_3)][NO_3]$,[22] the Zr is eight-coordinate and the Zr–O(nitrato) distances are 2.340(3) and 2.399(4) Å. In the complex anion $[L_{OEt}Zr(NO_3)_2(SO_4)]^-$, the nitrato ligands bind to Zr in an asymmetrical, bidentate fashion (average long and short Zr–O(nitrate) distances of 2.300(3) and 2.439(4) Å, respectively), whereas a more symmetrical binding mode was found for the chelating sulfato group (Zr–O distances of 2.164(4) and 2.232(3) Å). The asymmetric, bidentate binding mode for nitrato ligands is well documented and is attributed to the strain in the four-membered MO_2N ring.[33] The Zr–O(L_{OEt}) distances in **10** in the range of 2.099(3) to 2.177(3) Å are comparable to those in $[(L_{OEt})_4Zr_4(\mu_3\text{-}O)_2(\mu\text{-}OH)_4(H_2O)_2][NO_3]_4$.[22]

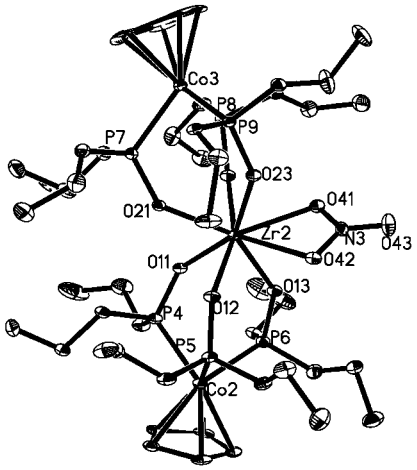

Figure 7. Molecular structure of the cation $[(L_{OEt})_2Zr(NO_3)]^+$ in **10**. The ellipsoids are drawn at 30% probability level. Selected bond lengths [Å] and angles [°]: Zr2–O(L_{OEt}) 2.099(3)–2.177(3) , Zr2–O41 2.340(3), Zr2–O42 2.399(4), O41–N3 1.269(6), O42–N3 1.281(5); O43-N3 1.202(5), O41-Zr2-O42 53.87(12).

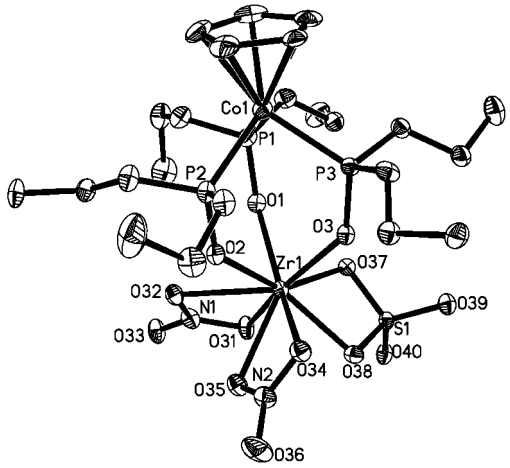

Figure 8. Molecular structure of the anion $[(L_{OEt})Zr(NO_3)_2(SO_4)]^-$ in **10**. The ellipsoids are drawn at 30% probability level. Selected bond lengths [Å] and angles [°]: Zr1–O(L_{OEt}) 2.114(3)–2.175(4), Zr1–O31 2.300(3), Zr1–O32 2.439(4), Zr1–O34 2.403(4), Zr1–O35 2.294(4), Zr1–O37 2.232(3), Zr1–O38 2.164(4), O31–N1 1.289(6), O32–N1 1.269(6), O33–N1 1.219(5), O35–N2 1.292(6), O36–N2 1.205(6), S1–O37 1.499(4), S1–O38 1.521(4), S1–O39 1.437(4), S1–O40 1.438(4); O31-Zr1-O32 53.98(13), O35-Zr1-O34 54.04(13), O38-Zr1-O37 62.77(13).

To prepare a nitrate-free $L_{OEt}Zr$ sulfato complex, $ZrCl_4$ was treated with NaL_{OEt} in sulfuric acid (ca. 1.8 M). Upon extraction with CH_2Cl_2 and recrystallization from CH_2Cl_2–hexane, yellow crystals of the sulfato-bridged dinuclear complex $[\{L_{OEt}Zr(SO_4)(H_2O)\}_2(\mu\text{-}SO_4)]\cdot 5H_2O$ (**11**·5 H_2O) were isolated (Scheme 4). The IR spectrum of **11** shows the S=O band at 1274 cm^{-1}. However, we were not able to determine whether this band is due to the chelate or bridging sulfato ligand. It may be noted that the symmetric O=S=O vibration for bidentate sulfate species on zirconia surfaces was observed in the range 1150–1250 cm^{-1}.[6] Complex **11** is air stable in CH_2Cl_2 but is somewhat hydroscopic in the solid state. In aqueous solution at pH 4, **11** shows a similar ^{31}P NMR spectrum to that of $[(L_{OEt})_4Zr_4(\mu_3\text{-}O)_2(\mu\text{-}OH)_4(H_2O)_2][NO_3]_4$ ($\delta = 121.9$ ppm),[22] suggesting that **11** hydrolyzed to tetranuclear $[(L_{OEt})_4Zr_4(\mu_3\text{-}O)_2(\mu\text{-}OH)_4(H_2O)_2]^{4+}$, which appears to be the most stable $L_{OEt}Zr^{IV}$ species in weakly acidic solution. The solid-state structure of **11**·5 H_2O consists of two $[L_{OEt}Zr(SO_4)(H_2O)]^+$ moieties bridged by a bidentate SO_4^{2-} ligand (Figure 9). The Zr–O distances for the bridging sulfato ligand (av 2.055(8) Å) are shorter than those for the chelate sulfato ligands (av 2.179 (8) Å), which are similar to those in **10**. The assignment of the oxygen atoms O14 and O19 as aqua ligands is consistent with the charge balance for the complex. The Zr–O(aqua) distances (av 2.217(8) Å) are comparable to those in $[(L_{OEt})_4Zr_4(\mu_3\text{-}O)_2(\mu\text{-}OH)_4(H_2O)_2][NO_3]_4$ (2.207(7) Å)[22] and $[ZrF_4(Me_2SO)(H_2O)_2]$ (2.220(2) Å),[34]

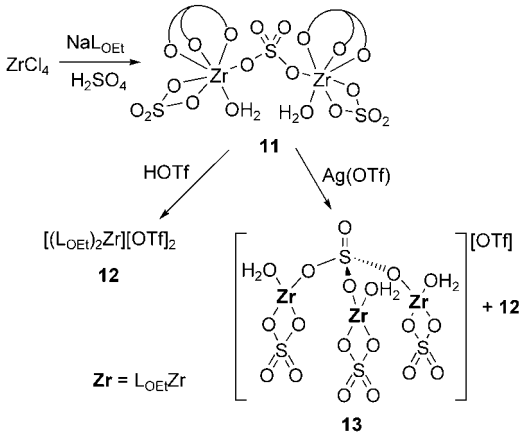

Scheme 4. Preparations of dinuclear and trinuclear Zr sulfato complexes.

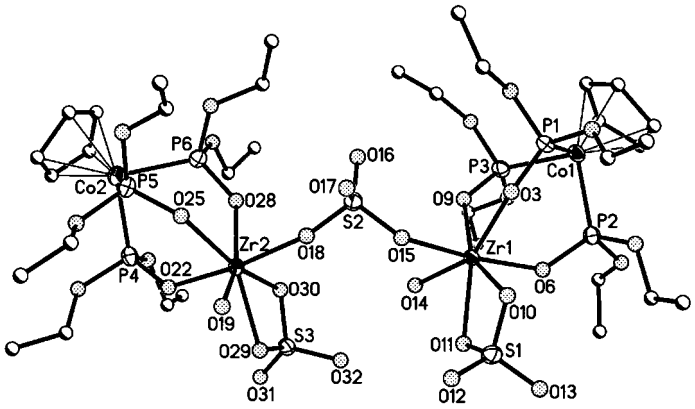

Figure 9. Molecular structure of **11**. The ellipsoids are drawn at 25% probability level. Selected bond lengths [Å] and angles [°]: Zr–O(L_{OEt}) 2.076(7)–2.146(7), Zr–O(bridging sulfate) 2.151(7)–2.210(7), Zr1–O14 2.248(8), Zr1–O15 2.063(8), Zr2–O18 2.047(8), Zr2–O19 2.187(7), S–O(Zr) (chelate) 1.495(8)–1.517(8), S–O_t (chelate) 1.412(9)–1.451(8), S2–O15 1.489(9), S2–O16 1.423(9), S2–O17 1.419(9), S2–O18 1.486(8); O11-Zr1-O10 63.9(3), O30-Zr2-O29 53.4(3), S2-O15-Zr1 152.7(5), S2-O18-Zr2 168.2(5).

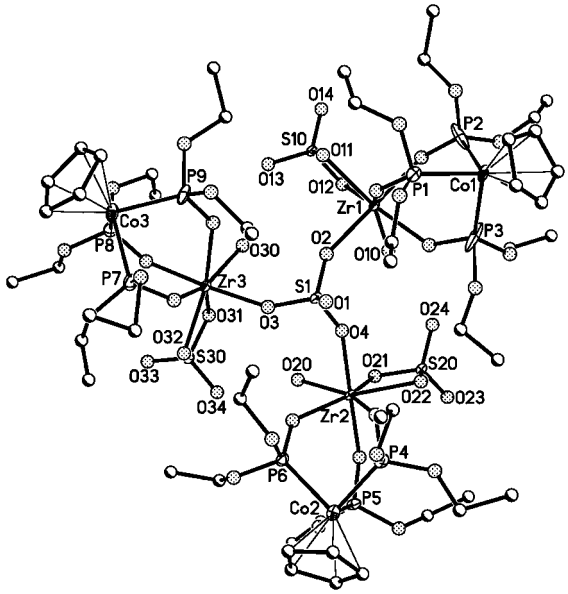

Figure 10. Molecular structure of the cation $[\{L_{OEt}Zr(SO_4)(H_2O)\}_3(\mu_3\text{-}SO_4)]^+$ in **13**.

but longer than typical terminal Zr–OH distances (e.g. 2.124 and 2.152 Å in $[Zr(OH)_2(CrO_4)]$.[35]

In an attempt to prepare a Zr analogue of **4**, **11** in CH_2Cl_2 was treated with triflic acid. However, instead of the triflato complex, the bis(tripod) complex $[(L_{OEt})_2Zr][OTf]_2$ (**12**) was isolated. Sulfate abstraction of **11** with Ag(OTf) in CH_2Cl_2 afforded a mixture of **12** and the trinuclear sulfato complex $[\{L_{OEt}Zr(H_2O)(SO_4)\}_3(\mu_3\text{-}SO_4)][OTf]$ (**13**) (Scheme 4). The IR S=O bands for the sulfato ligands and triflate ion were observed at 1261 and 1290 cm^{-1}, respectively. Compound **13** has been unambiguously characterized by an X-ray diffraction study. The structure of the cation $[\{L_{OEt}Zr(H_2O)(SO_4)\}_3(\mu_3\text{-}SO_4)]^+$ in **13**, which consists of three $[L_{OEt}Zr(SO_4)(H_2O)]^+$ cationic moieties bridged by a tridentate SO_4^{2-} ligand, is shown in Figure 10. While the identity of the trinuclear core in **13** has been confirmed, its bond lengths and angles have not been analyzed given the high *R* values due to the disorder of the structure.

Finally, it was found that the triflato compound $[L_{OEt}Zr(OTf)_3]$ (**14**) could be synthesized by reaction of $[L_{OEt}ZrF_3]$[21] with Me_3SiOTf in CH_2Cl_2, a method that has been used for the preparation of $[Cp^*_2Zr(OTf)_2]$.[36] The ^{19}F resonance for the triflato ligands in **14** ($\delta = -78.5$ ppm) is similar to that for **4** but more upfield than that for $[Cp^*_2Zr(OTf)_2]$ ($\delta = -75.8$ ppm).[36] Like other Ti^{IV} and Zr^{IV} triflato compounds, **4** and **14** are Lewis acidic and can catalyze organic reactions. For example, in the presence of 0.5 mol% of **4**, 1,3-cyclohexadiene reacted with acrolein in 30 min to afford the Diels–Alder product in 83% yield and an *endo*:*exo* ratio of about 95:5 (Scheme 5). A slightly lower yield was found for the Zr catalyst **14** (68% yield, *endo*:*exo* ratio of ca. 90:10). The reactivity and selectivity of the L_{OEt}-based catalysts are comparable to those for the metallocene analogues $[Cp_2M(OTf)_2]$.[37] Efforts are being made to explore other catalytic activity of the Ti and Zr triflato complexes.

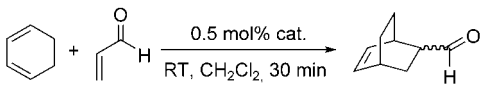

cat.	yield (%)	*endo*:*exo*
4	85	95:5
14	68	90:10

Scheme 5. Ti- and Zr-catalyzed Diels–Alder reaction.

Conclusion

In summary, we have synthesized and structurally characterized dinuclear and trinuclear Ti^{IV} and Zr^{IV} compounds containing chelating and bridging sulfato ligands in oxygen-only coordination environments. The core structures of these compounds are relevant to the proposed models of sulfated zirconia active sites. We found that the in aqueous solution, the $[Ti_2(\mu\text{-}O)_2(\mu\text{-}SO_4)]$ and $[Ti_2(\mu\text{-}O)(\mu\text{-}SO_4)_2]$ cores could be interconverted to each other. In CH_2Cl_2 solution, facile Ag(OTf)-induced conversion of bidentate to tridentate sulfato ligand in the Ti and Zr sulfato complexes, that is, the $[Ti_2(\mu\text{-}O)_2(\mu\text{-}SO_4)] \rightarrow [Ti_3(\mu\text{-}O)_3(\mu_3\text{-}SO_4)]$ and $[Zr_2(SO_4)_2(\mu\text{-}SO_4)] \rightarrow [Zr_3(SO_4)_3(\mu_3\text{-}SO_4)]$ conversions, was observed. It may be noted that the change in binding mode from bidentate to tridentate has been suggested to occur for the surface sulfato group when the calcination temperature of sulfated zirconia is increased from 673 to 923 K.[6a,8] The Ti^{IV} sulfato compound **2** can serve as a building block for heterometallic sulfato-bridged compounds. In the Ru/Ti compound **9**, the

$Ti_2O_2(\mu\text{-}SO_4)$ core acts as a tridentate, dianionic ligand that binds to Ru in a *fac-O,O,O*(SO_4) fashion. Whether such a binding mode may play a role in bifunctional M/sulfated zirconia catalysts is not clear. In addition, we found that the triflato complexes **4** and **14** are Lewis acidic and capable of catalyzing organic reactions such as the Diels–Alder reaction. Thus, it may be possible to model zirconia-based acid-catalyzed reactions using oxygen-rich L_{OEt}–Ti and L_{OEt}–Zr complexes. Currently, efforts are being made to investigate the interactions between transition metal alkyls and hydrides and L_{OEt}–Ti and L_{OEt}–Zr sulfato compounds, which may provide insight into mechanisms of organometallic reactions occurring on sulfated zironia surfaces.

Experimental Section

General procedures: Unless otherwise stated, all reactions were carried out in air. NMR spectra were recorded on a Bruker ALX 300 spectrometer operating at 300, 75, 282.5, and 121.5 MHz for ^{1}H, ^{13}C, ^{19}F, and ^{31}P, respectively. Chemical shifts (δ, ppm) were reported with reference to $SiMe_4$ (^{1}H and ^{13}C), $CF_3C_6H_5$ (^{19}F), and 85% H_3PO_4 (^{31}P). Infrared spectra (KBr) were recorded on a Perkin-Elmer 16 PC FT-IR spectrophotometer and mass spectra on a Finnigan TSQ 7000 (FAB) and Applied Biosystem QSTAR (ESI) spectrometer. Elemental analyses were performed by Medac Ltd, Surrey, UK.

The ligand NaL_{OEt},[38] [{Rh(cod)Cl}$_2$],[39] [Ru(*t*Bu$_2$bpy)(PPh$_3$)$_2$Cl$_2$],[30] and [$L_{OEt}ZrF_3$][21] were prepared according to literature methods. Titanyl sulfate (~15 wt% in dilute sulfuric acid) and zirconyl nitrate (~35 wt% in dilute nitric acid) were obtained from Aldrich and used as received. A stock solution of titanyl sulfate in sulfuric acid ([Ti] ~ 0.13 M) was freshly prepared by diluting commercial titanyl sulfate (Aldrich; 1 mL) with distilled water (9 mL) and used for the following preparations.

[(L_{OEt}Ti)$_2$(μ-O)$_2$(μ-SO$_4$)] (2): To the stock solution of titanyl sulfate (1.0 mL, 0.095 mmol) were added water (7 mL) and NaL_{OEt} (48 mg, 0.086 mmol) in water (3 mL). The mixture was stirred at room temperature for 10 min and Na_2SO_4 (60 mg, 0.423 mmol) in water (1 mL) was added. The resulting solution was stirred for 2 h, extracted with CH_2Cl_2 (2 × 10 mL), and dried with anhydrous Na_2SO_4. The solvent was removed in vacuo and the residue was recrystallized from acetone–hexane to afford yellow crystals that were suitable for X-ray analysis. Yield: 56 mg (50%). ^{1}H NMR (300 MHz, [D$_6$]acetone, 25°C, TMS): δ = 1.43 (t, J(H,H) = 7 Hz, 36H; CH_3), 4.28 (m, 24H; OCH_2), 5.30 ppm (s, 10H; Cp); ^{31}P {^{1}H} NMR (121.5 MHz, [D$_6$]acetone, 25°C, H_3PO_4): δ = 119.3 ppm (m); ^{31}P {^{1}H} NMR (121.5 MHz, $CDCl_3$, 25°C, H_3PO_4): δ = 119.0 ppm (m); ^{31}P {^{1}H} NMR (121.5 MHz, D_2O, pD ~0.5, 25°C, H_3PO_4): δ = 123.2 (d, J(P,P) = 1.3 Hz), 131.1 ppm (t, J(P,P) = 1.2 Hz); IR (KBr): $\tilde{\nu}$ = 1259 cm^{-1} (S=O); MS (FAB): m/z: 1294 [M]$^+$; elemental analysis calcd (%) for $C_{34}H_{70}Co_2O_{24}P_6STi_2$: C 31.5, H 5.45; found: C 31.5, H 5.41.

[(L_{OEt})$_2$Ti$_2$(μ-SO$_4$)$_2$(μ-O)] (3): To the titanyl sulfate stock solution (0.64 mL, 0.06 mmol) were added 10% H_2SO_4 (10 mL) and NaL_{OEt} (30 mg, 0.054 mmol) in water (3 mL). The mixture was stirred for 5 min and concentrated H_2SO_4 (0.48 g) was added. The resulting solution was stirred for 2 h, extracted with CH_2Cl_2 (2 × 10 mL), and dried over anhydrous Na_2SO_4. The solvent was removed in vacuo. Recrystallization from THF–hexane afforded yellow crystals, which were suitable for X-ray analysis. Yield: 36 mg (48%). ^{1}H NMR (300 MHz, [D$_6$]acetone, 25°C, TMS): δ = 1.50 (t, J(H,H) = 7 Hz, 36H; CH_3), 4.28–4.44 (m, 24H; OCH_2), 5.38 ppm (s, 10H; Cp); ^{31}P {^{1}H} NMR (121.5 MHz, [D$_6$]acetone, 25°C, H_3PO_4): δ = 120.6 (t, J(P,P) = 1.3 Hz), 125.9 ppm (d, J(P,P) = 1.3 Hz); ^{31}P {^{1}H} NMR (121.5 MHz, $CDCl_3$, 25°C, H_3PO_4): δ = 119.4 (t, J(P,P) = 1.1 Hz), 125.8 ppm (d, J(P,P) = 1.1 Hz); ^{31}P {^{1}H} NMR (121.5 MHz, D_2O, pD ~0.5, 25°C, H_3PO_4): δ = 124.5 (t, J(P,P) = 1 Hz), 131.5 ppm (d, J(P,P) = 1 Hz); IR (KBr): $\tilde{\nu}$ = 1281 cm^{-1} (S=O); elemental analysis calcd (%) for $C_{34}H_{70}Co_2O_{27}P_6S_2Ti_2{\cdot}CH_2Cl_2$: C 28.0 H, 4.83; found: C 27.8, H 4.75.

[L_{OEt}Ti(OTf)$_3$] (4): To a solution of **2** (40 mg, 0.03 mmol) in CH_2Cl_2 (10 mL) at −40°C was added triflic acid (0.05 mL) under nitrogen. The reaction mixture was slowly warmed to room temperature at which it was stirred for 2 h. To the resulting orange solution was added Et_2O/hexane (1:1) until an orange precipitate was formed. The solid was collected and recrystallized from CH_2Cl_2–Et_2O–hexane under nitrogen to give orange crystals that were suitable for X-ray diffraction. Yield: 31 mg (48%). ^{1}H NMR (300 MHz, $CDCl_3$, 25°C, TMS): δ = 1.39 (t, J(H,H) = 7 Hz, 18H; CH_3), 4.33–4.43 (m, 12H; CH_2), 5.34 ppm (s, 5H; Cp); ^{19}F {^{1}H} NMR (282.5 MHz, $CDCl_3$, 25°C, $CF_3C_6H_5$): δ = −77.7 ppm (s); ^{31}P {^{1}H} NMR (121.5 MHz, $CDCl_3$, 25°C, H_3PO_4): δ = 134.0 ppm (s); elemental analysis calcd (%) for $C_{20}H_{35}CoF_9O_{18}P_3S_3Ti$: C 23.3, H 3.39; found: C 23.4, H 3.49.

[(L_{OEt})$_3$Ti$_3$(μ-O)$_3$(μ_3-SO$_4$){Ag(OTf)}][OTf] (5): To a solution of **2** (76 mg, 0.06 mmol) in CH_2Cl_2 (10 mL) was added AgOTf (60 mg, 0.23 mmol), and the mixture was stirred at room temperature for 2 h. The volatiles were removed in vacuo and the residue was extracted into toluene. Recrystallization from THF–hexane afforded pale yellow crystals that were suitable for X-ray diffraction. Yield: 27 mg (30%). ^{1}H NMR (300 MHz, $CDCl_3$, 25°C, TMS): δ = 1.31 (t, J(H,H) = 7 Hz, 54H; CH_3), 3.90–4.04 (m, 6H; CH_2), 4.05–4.20 (m; 24H, CH_2), 4.21–4.38 (m, 6H; CH_2), 5.10 ppm (s, 15H; Cp); ^{19}F {^{1}H} NMR (282.5 MHz, $CDCl_3$, 25°C, $CF_3C_6H_5$): δ = −78.2 ppm (s); ^{31}P {^{1}H} NMR (121.5 MHz, $CDCl_3$, 25°C, H_3PO_4): δ = 120.9 (d, J(P,P) = 1.2 Hz), 129.2 ppm (t, J(P,P) = 1.2 Hz); MS (FAB): m/z: 2044 [M−AgOTf]$^+$, 1894 [M−AgOTf−OTf]$^+$; IR (KBr): $\tilde{\nu}$ = 1263 cm^{-1} (S=O); elemental analysis calcd (%) for $C_{53}H_{105}AgCo_3F_6O_{40}P_9S_3Ti_3$: C 27.6, H 4.60; found: C 27.8, H 4.75.

[(L_{OEt}Ti)$_4$(μ-O)$_6$]·1.5 HNO$_3$ (6·1.5 HNO$_3$): $Ba(NO_3)_2$ (11.4 mg, 0.044 mmol) in water (4 mL) was added dropwise to an aqueous solution (30 mL) of **2** (30 mg, 0.022 mmol), and the mixture was stirred in air at room temperature for 30 min. The solution was filtered, extracted into CH_2Cl_2, and evaporated to dryness. Recrystallization from CH_2Cl_2–hexanes gave yellow crystals. Yield: 13 mg (25%). ^{1}H NMR (300 MHz, $CDCl_3$, 25°C, TMS): δ 1.28 (t, J(H,H) = 9 Hz), 72H; CH_3), 3.93–4.23 (m, 48H; OCH_2), 5.08 ppm (s, 20H; Cp); ^{31}P {^{1}H} NMR (121.5 MHz, $CDCl_3$, 25°C, TMS): δ 122.5 ppm (s); elemental analysis calcd (%) for $C_{68}H_{140}Co_4O_{42}P_{12}Ti_4{\cdot}1.5\,HNO_3{\cdot}2\,H_2O$: C 31.0, H 5.88, N 0.80; found: C 30.78, H 5.58, N 0.77; MS (ESI): m/z: 1214.966 [M + 1]$^{2+}$.

[(L_{OEt}Ti)$_2$(O)$_2$(SO$_4$){Rh(cod)}$_2$][OTf]$_2$ (7): A mixture of **2** (30 mg, 0.022 mmol), [{Rh(cod)Cl}$_2$] (9.8 mg, 0.010 mmol), and AgOTf (10.2 mg, 0.020 mmol) in CH_2Cl_2 (5 mL) was stirred for at room temperature under nitrogen for 4 h and filtered. The orange filtrate was layered with hexane overnight to give orange needles. Yield: 15 mg (75%). ^{1}H NMR (300 MHz, $CDCl_3$, 25°C, TMS): δ = 1.22 (m, 8H; cod), 1.35 (m, 36H; CH_3), 1.64 (d, J(H,H) = 7.8 Hz, 4H; cod), 2.36 (m, 4H; cod), 4.01 (m, 8H; cod), 4.19 (m, 24H; CH_2), 5.24 ppm (s, 10H; Cp); ^{19}F {^{1}H} NMR (282.5 MHz, $CDCl_3$, 25°C, $CF_3C_6H_5$): δ = −78.5 ppm (s); ^{31}P {^{1}H} NMR (121.5 MHz, $CDCl_3$, 25°C, H_3PO_4): δ = 122.0 pm (m); IR (KBr): $\tilde{\nu}$ = 1275, 1265 cm^{-1} (S=O); elemental analysis calcd (%) for $C_{52}H_{94}Co_2F_6O_{30}P_6Rh_2S_3Ti_2$: C 31.0, H 4.70; found: C 30.9, H 5.21.

[(L_{OEt}Ti)$_2$(O)$_2$(SO$_4$){Re(CO)$_3$][OTf] (8): To solution of [Re(CO)$_5$Cl] (59 mg, 0.16 mmol) in CH_2Cl_2 (5 mL) was added AgOTf (46.6 mg, 0.18 mmol) under nitrogen, and the mixture was stirred for 2 h and filtered. To the filtrate was added **2** (109 mg, 0.08 mmol) and resulting solution was stirred at room temperature under nitrogen for three days. The volatiles were pumped off and the residue was extracted into Et_2O. Recrystallization from Et_2O–hexane afforded yellowish orange needles. Yield: 89.0 mg (63%). ^{1}H NMR (300 MHz, $CDCl_3$, 25°C, TMS): δ = 1.34 (t, 18H; CH_3), 4.27 (m, 12H; CH_2), 5.25 ppm (s, 5H; Cp); ^{19}F {^{1}H} NMR (282.5 MHz, $CDCl_3$, 25°C, $CF_3C_6H_5$): δ = −79.4 ppm (s); ^{31}P {^{1}H} NMR (121.5 MHz, $CDCl_3$, 25°C, H_3PO_4): δ = 119.4 (br. s), 125.6 (br. s), 128.2 ppm (d); IR (KBr): $\tilde{\nu}$ = 2025 cm^{-1} (C=O), 1278, 1294 cm^{-1} (S=O); MS (FAB): m/z: 1566 [M−OTf + 1]$^+$.

[{(L_{OEt})$_2$Ti$_2$(μ-O)}(μ_3-SO$_4$)(μ-O)$_2${Ru(*t*Bu$_2$bpy)(PPh$_3$)}][OTf]$_2$ (9): A mixture of [Ru(*t*Bu$_2$bpy)(PPh$_3$)$_2$Cl$_2$] (29.3 mg, 0.04 mmol) and AgOTf (40.0 mg, 0.16 mmol) in CH_2Cl_2 (20 mL) was stirred at room temperature

under nitrogen for 1 h and filtered. To the filtrate was added **2** (77.9 mg, 0.06 mmol) and the brown mixture was stirred overnight and evaporated to dryness. Recrystallization from CH_2Cl_2–hexane afforded reddish brown needles that were suitable for X-ray analysis. Yield: 49 mg (50 %). μ_{eff} (solid, 25 °C) = 2.40 μ_B; IR (KBr): $\tilde{\nu}$ = 1271 cm^{-1} (S=O); MS (FAB): *m/z*: 1944 $[M-2OTf]^+$; $E_{1/2}$ (0.1 M $[nBu_4N][PF_6]$ in CH_2Cl_2, glassy carbon electrode, scan rate = 100 mV s^{-1}) = +0.04 V versus $Cp_2Fe^{+/0}$; elemental analysis calcd (%) for $C_{72}H_{109}N_2O_{31}P_7S_3F_6Co_2Ti_2Ru{\cdot}4H_2O$: C 37.4, H 5.10, N 1.21; found: C 37.8, H 5.12, N 1.17.

$[(L_{OEt})_2Zr(NO_3)][(L_{OEt})Zr(NO_3)_2(SO_4)]$ (10): To zirconyl nitrate (0.7 mL of a 3.5 wt % solution, Aldrich, 0.107 mmol) was added H_2SO_4 (20 %, 10 mL) and NaL_{OEt} (53 mg, 0.095 mmol) in water (3 mL) and the reaction mixture was stirred at room temperature for 10 min. The solution was extracted into CH_2Cl_2, dried over anhydrous Na_2SO_4, and evaporated to dryness. Recrystallization from acetone-hexane afforded yellow crystals that were suitable for X-ray analysis. Yield: 40 mg (41 %). ^1H NMR (300 MHz, [D_6]acetone, 25 °C, TMS): δ = 1.46 (t, *J*(H,H) = 7 Hz, 54 H; CH_3), 4.31 (m, 36 H; CH_2), 5.42 (s, 5 H; Cp), 5.46 ppm (s, 10 H; Cp); $^{31}P\{^1H\}$ NMR (121.5 MHz, [D_6]acetone, 25 °C, H_3PO_4): δ = 120.9 (m), 122.4 ppm (m); IR (KBr): $\tilde{\nu}$ = 1248 cm^{-1} (S=O); elemental analysis calcd (%) for $C_{51}H_{105}N_3Co_3O_{40}P_9SZr_2{\cdot}CH_2Cl_2{\cdot}5H_2O$: C 27.9, H 5.25, N 1.87; found: C 28.4, H 5.17, N 1.47.

$[L_{OEt}Zr(H_2O)(SO_4)]_2(\mu\text{-}SO_4){\cdot}5H_2O$ (11·5 H_2O): A stock solution of "zirconyl sulfate" in H_2SO_4 was prepared by dissolving $ZrCl_4$ (0.5 g) in 10 % H_2SO_4 (10 mL). To the "zirconyl sulfate" stock solution (0.5 mL, [Zr] ~0.1 mmol) was added NaL_{OEt} (48 mg, 0.086 mmol) in water (20 mL), and the mixture was stirred at room temperature for 5 min. Then concentrated H_2SO_4 (0.5 mL) was added and the solution was stirred for 2 h and extracted with CH_2Cl_2. The organic layer was dried over Na_2SO_4 and evaporated to dryness. Recrystallization from THF–hexane afforded yellow blocks suitable for X-ray crystallography. ^1H NMR (300 MHz, [D_6]acetone, 25 °C, TMS): δ = 1.44 (t, *J*(H,H) = 7 Hz, 36 H; CH_3), 4.37 (m, 24 H; CH_2), 5.40 ppm (s, 10 H; Cp); $^{31}P\{^1H\}$ NMR (121.5 MHz, [D_6]acetone, 25 °C, H_3PO_4):δ = 121.1 ppm (m); IR (KBr): $\tilde{\nu}$ = 1274 cm^{-1} (S=O); elemental analysis calcd (%) for $C_{34}H_{72}Cl_2Co_2O_{30}P_6S_3Zr_2{\cdot}2(Me_2CO){\cdot}5H_2O$: C 26.9 H, 5.43; found: C 26.8, H 5.79.

$[(L_{OEt})_2Zr][OTf]_2$ (12): To a solution of **11**·5 H_2O (43 mg, 0.025 mmol) in CH_2Cl_2 (20 mL) was added triflic acid (0.05 mL) at −78 °C under nitrogen. The mixture was slowly warmed to room temperature and stirred for 1 h. The volatiles were pumped off and the residue washed with hexane. Recrystallization from CH_2Cl_2–hexane afforded yellow crystals. Yield: 11 mg (30 %). ^1H NMR (300 MHz, $CDCl_3$, 25 °C, TMS): δ = 1.35 (t, *J*(H,H) = 7 Hz, 36 H; CH_3), 4.16 (m, 24 H; CH_2), 5.31 ppm (s, 10 H; Cp); $^{31}P\{^1H\}$ NMR (121.5 MHz, $CDCl_3$, 25 °C, H_3PO_4): δ = 124.5 ppm (m); MS (FAB): *m/z*: 1160 $[M-2OTf]^+$.

Reaction of 11·5 H_2O with Ag(OTf): To **11**·5 H_2O (48.8 mg, 0.029 mmol) in CH_2Cl_2 at 0 °C was added two equivalents of Ag(OTf), and the mixture was stirred at room temperature for 1 h. After filtration and extraction with CH_2Cl_2, an inseparable mixture of **12** and $[\{L_{OEt}Zr(SO_4)(H_2O)\}_3(\mu_3\text{-}SO_4)][OTf]$ (**13**) (in 3:2 ratio, according to NMR spectroscopy) was isolated. Recrystallization from CH_2Cl_2–hexane gave a small amount of single crystals of **13** that were subjected to an X-ray diffraction study. Spectroscopic data for **13**: ^1H NMR (300 MHz, $CDCl_3$, 25 °C, TMS): δ = 1.29 (t, *J*(H,H) = 7 Hz, 54 H; CH_3), 4.18 (m, 36 H; CH_2), 5.42 ppm (s, 15 H; Cp); $^{31}P\{^1H\}$ NMR (121.5 MHz, $CDCl_3$, 25 °C, H_3PO_4): δ = 122.4 ppm (m); IR (KBr): $\tilde{\nu}$ = 1261, 1290 cm^{-1} (S=O).

$[L_{OEt}Zr(OTf)_3]$ (14): To a solution (8 mL) of $[L_{OEt}ZrF_3]$ (80 mg, 0.117 mmol) in CH_2Cl_2 in a flame-dried Schlenk was added Me_3SiOTf (70 μL, 0.39 mmol) under nitrogen, and the mixture was stirred at room temperature. The reaction was complete in about 2 h according to ^{19}F and ^{31}P NMR spectroscopy (δ = −175.4 and 121.5 ppm, respectively). The volatiles were pumped off and the residue washed with hexanes. Recrystallization from THF–hexane gave a yellow crystalline solid. Yield: 75 mg (60 %). ^1H NMR (300 MHz, $CDCl_3$, 25 °C, TMS): δ 1.37 (t, *J*(H,H) = 7 Hz, 18 H, CH_3), 4.17 (m, 12 H, OCH_2), 5.34 ppm (s, 5 H, C_5H_5); $^{31}P\{^1H\}$ NMR (121.5 MHz, $CDCl_3$, 25 °C, H_3PO_4), δ 127.7 ppm (m); $^{19}F\{^1H\}$ NMR (282.5 MHz, $CDCl_3$, 25 °C, $CF_3C_6H_5$): δ −78.5 ppm (s); elemental analysis calcd (%) for $C_{20}H_{35}CoF_9O_{18}P_3S_3Zr{\cdot}C_4H_{10}O{\cdot}0.5\,C_6H_{14}{\cdot}4H_2O$: C 25.7, H 4.64; found: C 25.7, H 4.76.

Catalytic Diels–Alder reaction of acrolein with 1,3-cyclohexadiene: To a solution of **4** or **14** (2.4 mol) in CH_2Cl_2 (1 mL) were added successively acrolein (32 μL, 0.48 mmol) and 1,3-cyclohexadiene (40 μL, 0.48 mmol) under nitrogen, and the mixture was stirred at room temperature for 30 min. The organic products were analyzed by GLC with a HP-1 column and quantified by internal standard method.

X-ray crystallography: Crystal data collection and refinement are summarized in Table 1 and Table 2. Preliminary examinations and intensity data collection were carried out on a Bruker SMART-APEX 1000 area-detector diffractometer using graphite-monochromated $Mo_{K\alpha}$ radiation (λ = 0.70173 Å). The collected frames were processed with the software SAINT.[40] The data was corrected for absorption using the program SADABS.[41] Structures were solved by direct methods and refined by full-matrix least-squares on F^2 using the SHELXTL software package.[42] Unless stated otherwise, non-hydrogen atoms were refined with anisotropic displacement parameters. Carbon-bonded hydrogen atoms were included in calculated positions and refined in the riding mode using

Table 1. Crystallographic data and experimental details for $[\{L_{OEt}Ti\}_2(\mu\text{-}O)_2(\mu\text{-}SO_4)]{\cdot}1.5H_2O$ (**2**·1.5 H_2O), $[\{L_{OEt}Ti\}_2(\mu\text{-}O)(\mu\text{-}SO_4)_2]{\cdot}1.5H_2O$ (**3**·1.5 H_2O), $[L_{OEt}Ti(OTf)_3]$ (**4**) and $[\{L_{OEt}Ti\}_3(\mu\text{-}O)_3(\mu_3\text{-}SO_4)\{AgOTf\}][OTf]$ (**5**).

	2·1.5 H_2O	**3**·1.5 H_2O	**4**	**5**
formula	$C_{34}H_{74}Co_2O_{25.5}P_6STi_2$	$C_{34}H_{74}Co_2O_{28.5}P_6STi_2$	$C_{20}H_{35}CoF_9O_{18}P_3S_3Ti$	$C_{53}H_{105}AgCo_3FO_{40}P_9S_3$
M_r	1330.47	1410.53	1030.40	2299.64
a [Å]	10.1917(5)	14.4929(5)	11.849(2)	16.511(1)
b [Å]	18.3201(9)	19.3251(7)	17.180(3)	16.587(1)
c [Å]	15.2348(8)	23.3879(8)	19.180(4)	20.239(1)
α [°]	90	90	90	86.440(1)
β [°]	106.583(1)	90	95.00(3)	68.192(1)
γ [°]	90	90	90	61.172(1)
V [Å^3]	2726.2(2)	6550.4(4)	3889.5(13)	4461.7(5)
Z	2	4	4	2
crystal system	monoclinic	orthorhombic	monoclinic	triclinic
space group	$P2_1$	$P2_12_12_1$	$P2_1/n$	$P\bar{1}$
ρ_{calcd} [g cm^{-3}]	1.621	1.430	1.760	1.712
T [K]	100(2)	100(2)	100(2)	100(2)
μ [mm^{-1}]	1.175	0.964	1.028	1.342
F(000)	1380	2598	2088	2348
no. of refln	16818	34450	18601	39753
no. of indep.	10273	11476	6677	15008
R_{int}	0.0238	0.0577	0.0797	0.0426
*R*1, *wR*2 ($I > 2.0\sigma(I)$)	0.0715, 0.1773	0.0932, 0.2474	0.0479 0.0610	0.0465, 0.1073
*R*1, *wR*2 (all data)	0.0833, 0.1889	0.1508, 0.2898	0.0538, 0.0669	0.0695, 0.1137
GoF on F^2 [a]	1.012	1.054	0.957	1.042

[a] GoF = $[(\Sigma w|F_o| - |F_c|)^2/(N_{obs}-N_{param})]^{1/2}$.

Table 2. Crystallographic data and experimental details for $[\{(L_{OEt})_2Ti_2(O)\}(\mu_3\text{-}SO_4)(\mu\text{-}O)_2\{Ru(PPh_3)(t\text{Bu}_2\text{bpy})\}](OTf)_2$ (**9**), $[(L_{OEt})_2Zr(NO_3)][(L_{OEt})Zr(NO_3)_2(SO_4)]\cdot Me_2CO$ (**10**·Me_2CO), $[\{L_{OEt}Zr(H_2O)(SO_4)\}_2(\mu\text{-}SO_4)]\cdot 5H_2O$ (**11**·$5H_2O$), and $[\{L_{OEt}Zr(SO_4)(H_2O)\}_3(\mu_3\text{-}SO_4)][OTf]\cdot 1.5H_2O$ (**13**·$1.5H_2O$).

	9	**10**·Me_2CO	**11**·$5H_2O$	**13**·$1.5H_2O$
formula	$C_{72}H_{109}Co_2F_6N_2O_{31}P_7RuS_3Ti_2$	$C_{54}H_{111}Co_3N_3O_{41}P_9SZr_2$	$C_{34}H_{86}Co_2O_{37}P_6S_3Zr_2$	$C_{52}H_{114}Co_3F_3O_{50.5}P_9S_5Zr_3$
M_r	2240.31	2128.48	1669.33	2493.91
a [Å]	27.617(2)	12.636(1)	18.323(1)	16.397(2)
b [Å]	16.934(1)	22.279(1)	19.305(1)	16.759(2)
c [Å]	20.620(1)	30.542(2)	19.150(2)	21.446(2)
α [°]	90	90	90	91.022(2)
β [°]	90	92.420(1)	95.937(2)	112.282(2)
γ [°]	90	90	90	115.332(2)
V [Å^3]	9642.8(9)	8590.5(9)	6737.6(9)	4813.2(7)
Z	4	4	4	2
crystal system	orthorhombic	monoclinic	monoclinic	triclinic
space group	$Pna2_1$	Cc	$P2_1/n$	$P\bar{1}$
ρ_{calcd} [g cm^{-3}]	1.543	1.646	1.646	1.721
T [K]	100(2)	100(2)	273(2)	100(2)
μ [mm^{-1}]	0.917	1.084	1.184	1.174
F(000)	4608	4384	3488	2546
no. of refln	50685	22554	33383	21600
no. of indep. refln.	16810	13833	11786	10356
R_{int}	0.0886	0.0235	0.1721	0.0796
$R1$, $wR2$	0.0689,	0.0382,	0.0619,	0.0900,
($I>2.0\sigma(I)$)	0.1494	0.0907	0.1315	0.1883
$R1$, $wR2$	0.1180,	0.0394,	0.2107,	0.1678,
(all data)	0.1678	0.0913	0.2333	0.2288
GoF on F^2[a]	1.001	1.093	0.848	1.068

[a] $GoF = [(\Sigma w |F_o| - |F_c|)^2/(N_{obs} - N_{param})]^{1/2}$

SHELXL97 default parameters. In **2**·$1.5H_2O$, **3**·$1.5H_2O$, **5**, **9**, and **11**·$5H_2O$, some of the ethoxy groups in the L_{OEt}^- ligands were disordered. In **1**·$1.5H_2O$, the phosphorus atoms in one L_{OEt}^- ligand were found to be disordered and the two sites were refined with occupancies 0.8 and 0.2. In **5**, the disordered Ag atom was refined with two sites Ag1A and Ag1B with occupancies of 0.8 and 0.2, respectively. Both the triflato ligand and triflate anion were also found to be disordered. The triflato ligand was refined with the carbon atom split into three sites C1A, C1B, and C1C with occupancies of 0.6, 0.25, and 0.15, respectively. In **9** and **13**·$1.5H_2O$, the triflate anions are disordered and were refined isotropically. CCDC-242961 (**2**·$1.5H_2O$), CCDC-242962 (**3**·$1.5H_2O$), CCDC-242963 (**4**), CCDC-242964 (**5**), CCDC-242965 (**9**), CCDC-242966 (**10**·Me_2CO)), CCDC-242967 (**11**·$5H_2O$), and CCDC-242968 (**13**·$1.5H_2O$) contain the supplementary crystallographic data for this paper. These data can be obtained free of charge via www.ccdc.cam.ac.uk/conts/retrieving.html (or from the Cambridge Crystallographic Data Centre, 12 Union Road, Cambridge CB2 1EZ, UK; fax: (+44) 1223-336-033; or deposit@ccdc.cam.ac.uk).

Acknowledgement

The work described in this paper was supported by a grant from the Hong Kong Research Grants Council of the Hong Kong Special Administrative Region, China (Project no. 602203).

[1] a) K. Arata, *Adv. Catal.* **1990**, *37*, 165; b) A. Corma, *Chem. Rev.* **1995**, *95*, 559; c) X. M. Song, A. Sayari, *Catal. Rev. Sci. Eng.* **1996**, *38*, 329; d) J. H. Clark, *Acc. Chem. Res.* **2002**, *35*, 791; e) A. Corma, H. Garcia, *Chem. Rev.* **2003**, *103*, 4307; f) G. D. Yadav, J. J. Nair, *Microporous Mesoporous Mater.* **1999**, *33*, 1; g) K. Arata, H. Matsuhashi, M. Hino, H. Nakamura, *Catal. Today* **2003**, *81*, 17.

[2] a) M. Hino, S. Kobayashi, K. Arata, *J. Am. Chem. Soc.* **1979**, *101*, 6439; b) M. Hino, K. Arata, *J. Chem. Soc. Chem. Commun.* **1980**, 851.

[3] a) K. Arata, H. Hino, *Shokubai* **1979**, *21*, 217; b) K. Ebitani, J. Konishi, H. Hattori, *J. Catal.* **1991**, *130*, 257; c) T. Kimura, *Catal. Today* **2003**, *81*, 57.

[4] a) H. Ahn, T. J. Marks, *J. Am. Chem. Soc.* **1998**, *120*, 13533; b) H. Ahn, C. P. Nicholas, T. J. Marks, *Organometallics* **2002**, *21*, 1788.

[5] K. Tanabe, T. Yamaguchi. *Catal. Today.* **1994**, *20*, 185.

[6] a) C. Morterra, G. Cerrato, F. Pinna, M. Signoretto, *J. Catal.* **1995**, *157*, 109; b) M. Bensitel, O. Saur, J.-C. Lavalley, B. A. Marrow, *Mater. Chem. Phys.* **1988**, *19*, 147.

[7] A. Davydov, *Molecular Spectroscopy of Oxide Catalyst Surfaces*, Wiley, Chichester, UK, **2003**, p. 286.

[8] F. Haase, J. Sauer, *J. Am. Chem. Soc.* **1998**, *120*, 13503.

[9] a) D. C. Bradley, R. C. Mehrotra, I. P. Rothwell, A. Singh, *Alkoxo and Aryloxo Derivatives of Metals*, Academic Press, San Diego, CA, **2001**; b) R. C. Mehrotra, A. Singh, *Prog. Inorg. Chem.* **1997**, *46*, 239; c) R. C. Mehortra, A. Singh, *Chem. Soc. Rev.* **1996**, *25*, 1; d) L. G. Hubert-Pfalzgraf, *Coord. Chem. Rev.* **1998**, *178–180*, 967.

[10] E. S. Johnson, G. J. Balaich, P. E. Fanwick, I. P. Rothwell, *J. Am. Chem. Soc.* **1997**, *119*, 11086.

[11] a) K. J. Covert, P. T. Wolczanski, *Inorg. Chem.* **1989**, *28*, 4565; b) K. J. Covert, P. T. Wolczanski, S. A. Hill, P. J. Krusic, *Inorg. Chem.* **1992**, *31*, 66.

[12] a) H. C. L. Abbenhuis, *Chem. Eur. J.* **2000**, *6*, 25; b) R. W. J. M. Hanssen, R. A. van Santen, H. C. L. Abbenhuis, *Eur. J. Inorg. Chem.* **2004**, 675; c) V. Lorenz, A. Fischer, S. Giessmann, J. W. Gilje, Y. Gun′ko, K. Jacob, F. T. Edelmann, *Coord. Chem. Rev.* **2000**, *206–207*, 321; d) R. Duchateau, *Chem. Rev.* **2002**, *102*, 3525.

[13] a) C. Floriani, R. Floriani-Moro, *Adv. Organomet. Chem.* **2001**, *47*, 167; b) O. V. Ozerov, F. T. Lapido, B. O. Patrick, *J. Am. Chem. Soc.* **1999**, *121*, 7941; c) A. J. Petrella, N. K. Roberts, C. L. Raston, M. Thornton-Pett, R. N. Lamb, *Chem. Commun.* **2003**, 1238; d) D. R. Evans, M. S. Huang, J. C. Fettinger, T. L. Williams, *Inorg. Chem.* **2002**, *41*, 5986; e) F. A. Cotton, E. V. Dikarev, C. A. Murillo, M. A. Petrukhina, *Inorg. Chim. Acta* **2002**, *332*, 41;

[14] a) F. Bottomley, L. Sutin, *Adv. Organomet. Chem.* **1988**, *28*, 339; b) H. W. Roesky, I. Haiduc, N. S. Hosmane, *Chem. Rev.* **2003**, *103*, 2579;

[15] a) A. Abarca, M. Galakhov, Gómez-Sal, A. Martín, M. Mena, J. M. Poblet, C. Santamaria, J. P. Sarasa, *Angew. Chem.* **2000**, *112*, 544; *Angew. Chem. Int. Ed.* **2000**, *39*, 534; b) J. Gracia, A. Martín, M. Mena, M. D. Morales-Varela, J. M. Poblet, C. Santamaría, *Angew. Chem.* **2003**, *115*, 957; *Angew. Chem. Int. Ed.* **2003**, *42*, 927; c) A. Martín, M. Mena, M. d. Morales-Varela, C. Santamaría, *Eur. J. Inorg. Chem.* **2004**, 1914.

[16] U. Thewalt, P. Schinnerling, *J. Organomet. Chem.* **1991**, *418*, 191.

[17] A. Abarca, A. Martín, M. Mena, P. R. Raithby, *Inorg. Chem.* **1995**, *34*, 5437.

[18] W. Kläui, *Angew. Chem.* **1990**, *102*, 661; *Angew. Chem. Int. Ed. Engl.* **1990**, *29*, 627.

[19] W. Kläui, A. Müller, W. Eberspach, R. Boese, I. Goldberg, *J. Am. Chem. Soc.* **1987**, *109*, 164.
[20] T. R. Ward, S. Duclos, B. Therrien, K. Schenk, *Organometallics* **1998**, *17*, 2490.
[21] T. C. H. Lam, E. Y. Y. Chan, W.-L. Mak, S. M. F. Lo, I. D. Williams, W.-T. Wong, W.-H. Leung, *Inorg. Chem.* **2003**, *42*, 1842.
[22] Q. F. Zhang, T. C. H. Lam, E. Y. Y. Chan, S. M. F. Lo, I. D. Williams, W. H. Leung, *Angew. Chem.* **2004**, *116*, 1747; *Angew. Chem. Int. Ed.* **2004**, *43*, 1715.
[23] K. Nakamoto, *Infrared and Raman Spectra of Inorganic and Coordination Compounds. Part B: Applications in Coordination, Organometallic, and Bioinorganic Chemistry*, 5th ed., Wiley, New York, **1997**, p. 79.
[24] U. Thewalt, D. Schomburg, *J. Organomet. Chem.* **1977**, *127*, 169.
[25] Y. Motoyama, M. Tanaka, K. Mikami, *Inorg. Chim. Acta* **1997**, *256*, 161.
[26] A preliminary X-ray diffraction study confirmed that **6** contains an adamantane-like Ti_4O_6 core similar to that in $[\{Cp^*Ti\}_4(\mu\text{-}O)_6]$ (ref. [27]). Unfortunately, we were not able to solve the crystal structure satisfactorily due to poor quality of the crystal. Crystal data: Hexagonal, $P\bar{3}c_1$, $a=29.9496(6)$, $b=23.7990(7)$, $V=18\,487.2(8)$ Å^3, $Z=3$, refinement converged to $R1=0.1688$, $wR2=0.3254$, and $S=1.498$ for 15 048 reflections and 349 variables.
[27] L. M. Babcock, V. W. Day, W. G. Kemperer, *J. Chem. Soc. Chem. Commun.* **1987**, 858.
[28] a) W. Clegg, R. J. Errington, D. C. R. Hockless, A. D. Glen, D. G. Richards, *J. Chem. Soc. Chem. Commun.* **1990**, 1565; b) R. L. Keiter, D. S. Strickland, S. R. Wilson, J. R. Shapley, *J. Am. Chem. Soc.* **1986**, *108*, 3846; c) J. Esteinne, R. Weiss, *J. Chem. Soc. Chem. Commun.* **1972**, 862; d) R. Beckett, B. F. Hoskins, *J. Chem. Soc. Dalton Trans.* **1972**, 291.
[29] R. Andrés, M. V. Galakhov, A. Martín, M. Mena, C. Santamaría, *Organometallics* **1994**, *13*, 2159.
[30] C. J. Adams, S. J. A. Pope, *Inorg. Chem.* **2004**, *43*, 3492.
[31] H. Nagao, M. Shibayama, Y. Kitanaka, F. S. Howell, K. Shimizu, M. Mukaida, H. Kakihana, *Inorg. Chim. Acta* **1991**, *185*, 75.
[32] J. M. Power, K. Evertz, L. Henling, R. Marsh, W. P. Schaefer, J. A. Labinger, J. E. Bercaw, *Inorg. Chem.* **1990**, *29*, 5058.
[33] B. J. Hathway in *Comprehensive Coordination Chemistry, Vol. 2* (Eds.: G. Wilkinson, R. D. Guilard, J. A. McCleverty) Pergamon, Oxford, **1987**, Chap. 15.5.
[34] C. Jacoboni, Y. Gao, J. Guery, *Acta Crystallogr. Sect. C* **1993**, *49*, 963.
[35] V. Langer, B. M. Casari, *Acta Crystallogr. Sect. C* **2000**, *C56*, e36.
[36] H. Dorn, S. A. A. Shah, M. Notlemeyer, H.-G. Schmidt, H. W. Roesky, *J. Fluorine Chem.* **1998**, *88*, 195.
[37] T. K. Hollis, N. P. Robinson, B. Bosnich, *Organometallics* **1992**, *11*, 2745.
[38] W. Kläui, *Z. Naturforsch. B* **1979**, *34*, 1403.
[39] G. Giodano, R. H. Crabtree, *Inorg. Synth.* **2000**, *28*, 88.
[40] Bruker SMART and SAINT+, Version 6.02a, Siemens Analytical X-ray Instruments Inc., Madison, Wisconsin, USA, **1998**.
[41] G. M. Sheldrick, SADABS, University of Göttingen, Germany, **1997**.
[42] G. M. Sheldrick, *SHELXTL-Plus V5.1 Software Reference Manual*; Bruker AXS Inc., Madison, Wisconsin, USA, **1997**.

Received: August 17, 2004
Published online: November 10, 2004

